

# SYNTHESIS, CHARACTERIZATION AND INFLUENCE OF CALCINATIONS TEMPERATURE ON MAGNETIC PROPERTIES OF $\text{Ni}_{0.75}\text{Zn}_{0.25}\text{Fe}_2\text{O}_4$ NANOPARTICLES SYNTHESIZED BY SOL-GEL TECHNIQUE

Beh Hoe Guan, Lee Kean Chuan and Hassan Soleimani

Department of Fundamental and Applied Sciences,  
Universiti Teknologi Petronas, Bandar Seri Iskandar, 31750 Tronoh Perak, Malaysia

Received 2013-11-12; Revised 2013-11-15; Accepted 2014-03-21

## ABSTRACT

The calcinations temperature is one of the important process parameter which influences the changes of magnetic properties in ferrites. This study provide better understanding of the influence of calcination temperatures on the magnetic properties of Nickel Zinc ferrite consequently enable to tailor the magnetic properties of Nickel Zinc ferrite for specific application. Magnetic nanoparticles of Nickel Zinc ferrite were synthesized by sol-gel technique. Their crystallite size and the influence of calcinations temperature on magnetic properties were investigated by using X-Ray Diffraction (XRD) and Vibrating Sample Magnetometer (VSM). XRD results showed that the crystallization of the Nickel Zinc ferrite increased as the calcination temperature increased. The results showed that single phase of Nickel Zinc ferrite samples can be obtained at various calcination temperatures from 800 to 1100°C. All Nickel Zinc ferrite samples exhibited ferrimagnetic behavior. VSM results showed that the saturation magnetization and coercivity values strongly influenced by the calcination temperature.

**Keywords:** Nanoparticles, Ferrite, Sol-Gel, Magnetic

## 1. INTRODUCTION

Nickel Zinc (NiZn) ferrite is a ferrimagnetic materials which are widely used in electronic devices such as EMI suppressor and electromagnetic wave absorber due to their low initial permeability. NiZn ferrite belongs to a space group  $Fd\bar{3}m$  with the general formula  $\text{AB}_2\text{O}_4$  where A and B refer to tetrahedral and octahedral sites, respectively, in the fcc oxygen lattice (Gao *et al.*, 2013). In the spinel structure,  $\text{Zn}^{2+}$  ions are preferred occupy in tetrahedral (Meng *et al.*, 2012) while  $\text{Ni}^{2+}$  prefer octahedral site (Sutka *et al.*, 2012). Magnetic properties of NiZn are from the magnetic ions ( $\text{Fe}^{3+}$ ) located in tetrahedral and octahedral coordinated sites and their interaction with surrounding oxygen ions. These oxygen ions influence

the electronic configuration of the enclosed iron ions and provide the superexchange interaction between the irons in different sites.

The calcinations temperature also plays a crucial role in magnetic properties of ferrite (Ismail *et al.*, 2013). The degree of crystallinity was found increased with the increasing of sintering temperature. The temperature caused the aggregation of particles and formed the impurities phase (Vaqueiro *et al.*, 1997). The present of impurities cause the change in the structure and texture of crystal, which results in change in the magnetic properties (Beh *et al.*, 2009). It was found that the permeability of ferrite increase as the sintering temperatures increases. The increase of permeability is due to the increase of density and grain size (Islam, 2012). The grain size of ferrite is

**Corresponding Author:** Beh Hoe Guan, Department of Fundamental and Applied Sciences, Universiti Teknologi Petronas, Bandar Seri Iskandar, 31750 Tronoh Perak, Malaysia

temperature dependent. It was found that the grain size grow with the increase of sintering temperature. Ferrites with large average grain size exhibits higher initial permeability.

Sol-gel technique is one of the well-known techniques to prepare the nanoparticles (Pozo Lopez *et al.*, 2012). In this technique the reactant cations are allowed to mix in the atomic scale, thus homogeneity gel can be prepared. The lower crystalline temperature of the ferrite can be obtained due to the homogeneity gel prepared (Cheng *et al.*, 2009). Although there are some reports about magnetic properties of Ni-Zn ferrites, however, a systemic investigation about the influence of calcinations temperature on magnetic properties in NiZn Ferrite is still limited. In this study,  $\text{Ni}_{0.75}\text{Zn}_{0.25}\text{Fe}_2\text{O}_4$  nanoparticles were synthesized using Sol-gel Technique and their magnetic properties at different calcinations temperature were studied.

## 2. MATERIALS AND METHODS

Metal salts of Nickel (II) Nitrate ( $\text{Ni}(\text{NO}_3)_2 \cdot 6\text{H}_2\text{O}$ ), Zinc Nitrate ( $\text{Zn}(\text{NO}_3)_2$ ) and Iron (III) Nitrate ( $\text{Fe}(\text{NO}_3)_3 \cdot 9\text{H}_2\text{O}$ ) were separately dissolved in an aqueous solution of 1M citric acid. The resulting solutions were mixed and stirred at room temperature. The mixed solution was then heated at 50°C to form a gel. Once formed, the gel was then heated in a furnace at 110°C for 24h. The obtained solid was calcined at temperature of 700°C to 1100°C for 3h.

The materials phases analysis were obtained by using X-Ray Diffraction (XRD) with Philips X-Ray diffractometer using Cu  $K\alpha$  radiation with  $\lambda = 1.5418\text{\AA}$ . The crystalline size were calculated using Scherrer equation  $D = k\lambda/\beta\cos\theta$ , where 'D' is the crystalline size, 'k' is the shape factor, ' $\lambda$ ' is wavelength of X-Ray, ' $\beta$ ' is the full width half maximum and ' $\theta$ ' is diffraction angle. The magnetic measurements were conducted at room temperature using a Vibrating Sample Magnetometer (VSM) with a maximum magnetic field of 20000Oe.

## 3. RESULTS

**Figure 1** shows the XRD patterns of  $\text{Ni}_{0.75}\text{Zn}_{0.25}\text{Fe}_2\text{O}_4$  samples calcined at different temperatures. **Figure 2** shows the average crystallite size of the  $\text{Ni}_{0.75}\text{Zn}_{0.25}\text{Fe}_2\text{O}_4$  calcined at different temperatures. The average crystallite size was calculated from the full width at half-maximum of the (022), (113) and (004) planes of  $\text{Ni}_{0.75}\text{Zn}_{0.25}\text{Fe}_2\text{O}_4$  using Scherrer equation. Magnetic properties of the  $\text{Ni}_{0.75}\text{Zn}_{0.25}\text{Fe}_2\text{O}_4$  at different calcinations temperatures

were obtained by VSM measurement. **Figure 3** show hysteresis curves of  $\text{Ni}_{0.75}\text{Zn}_{0.25}\text{Fe}_2\text{O}_4$  calcined at different temperatures. The hysteresis curves show ferrimagnetic behavior. The saturation magnetisation and coecivity values of  $\text{Ni}_{0.75}\text{Zn}_{0.25}\text{Fe}_2\text{O}_4$  calcined at different temperatures are tabulated in **Table 1**.

## 4. DISCUSSION

At 700°C, the XRD diffractogram shows six peaks appeared at 30.26, 33.46, 35.61, 37.35, 43.54 and 62.72°. By matching with JCPDS diffraction data, it is determined that the peaks located at  $2\theta = 30.26, 35.61, 37.35, 43.54$  and  $62.72^\circ$  are corresponding to (022), (113), (004), (333) and (044) diffraction planes of cubical  $\text{Ni}_{0.75}\text{Zn}_{0.25}\text{Fe}_2\text{O}_4$  (JCPDS code 00-052-0277), respectively. The peak located at  $2\theta = 33.46^\circ$  is corresponding to (104) diffraction plane of  $\text{Fe}_2\text{O}_3$ . The existence of  $\text{Fe}_2\text{O}_3$  as an impurity phase suggesting that the thermal energy applied to the sample still not enough to form a single phase. The diminution of  $\text{Fe}_2\text{O}_3$  phase is observed upon increase the calcination temperature to 800°C. All the peaks appeared at this temperature can be completely indexed to the seven peaks of  $\text{Ni}_{0.75}\text{Zn}_{0.25}\text{Fe}_2\text{O}_4$  which are (022), (113), (222), (004), (333) and (044) diffraction planes. Therefore, it can be concluded that the calcination temperature to obtain a single phase of  $\text{Ni}_{0.75}\text{Zn}_{0.25}\text{Fe}_2\text{O}_4$  will be 800°C. At 800°C, the major peak of  $\text{Ni}_{0.75}\text{Zn}_{0.25}\text{Fe}_2\text{O}_4$  phase at  $33.56^\circ$  become stronger and impurity peak appeared at  $33.46^\circ$  diminished. This implies that amount of the crystallinity phase is increased with the increasing of calcinations temperature. Further increase the temperature to 900°C leads to the formation of more crystalline product, as can be seen from the sharp diffraction peaks correspond to  $\text{Ni}_{0.75}\text{Zn}_{0.25}\text{Fe}_2\text{O}_4$  appeared in the sample. As shown in **Fig. 1**, the intensity of the major peaks corresponds to  $\text{Ni}_{0.75}\text{Zn}_{0.25}\text{Fe}_2\text{O}_4$  further increase with the increasing of temperature up to 1100°C and starts to saturate at 1100°C. It is suggesting that the full crystallisation was achieved at a temperature of 1100°C.

As shown in the **Fig. 2**, it is observed that the average size of  $\text{Ni}_{0.75}\text{Zn}_{0.25}\text{Fe}_2\text{O}_4$  at 700°C is 24.9nm. The crystallite size increases to 55.5nm with the increasing in temperature from 700°C to 800°C. This can be attributed to the diminution of  $\text{Fe}_2\text{O}_3$  phase in the sample. Further increases the temperature to 1000°C, it was found that the crystallite size of  $\text{Ni}_{0.75}\text{Zn}_{0.25}\text{Fe}_2\text{O}_4$  decreases to 32.5nm.

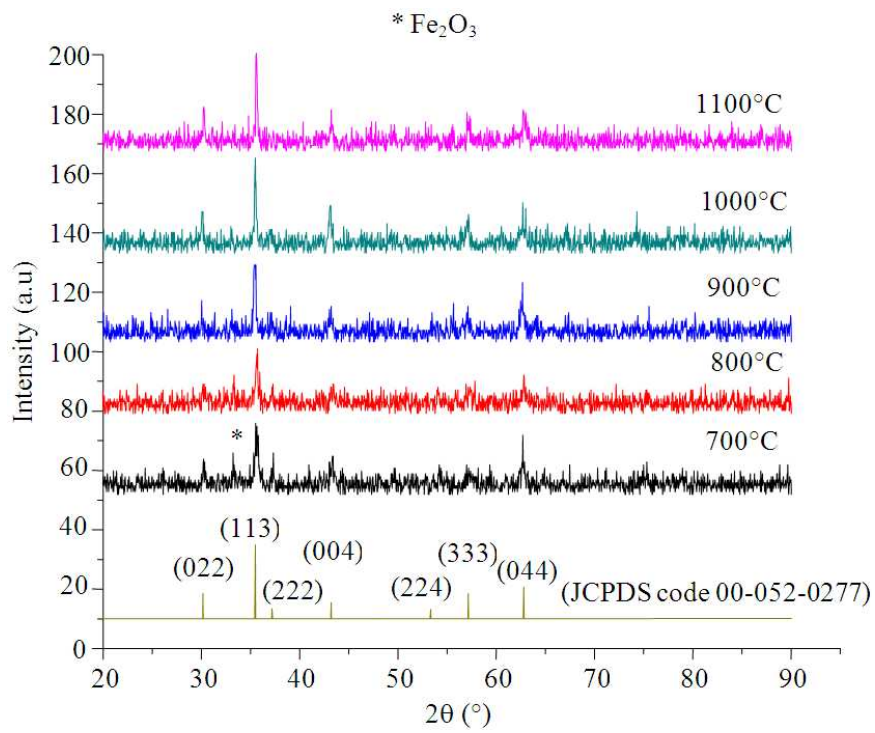


**Fig. 1.** XRD Patterns of Ni<sub>0.75</sub>Zn<sub>0.25</sub>Fe<sub>2</sub>O<sub>4</sub> calcined at different temperatures from 700°C to 1100°C

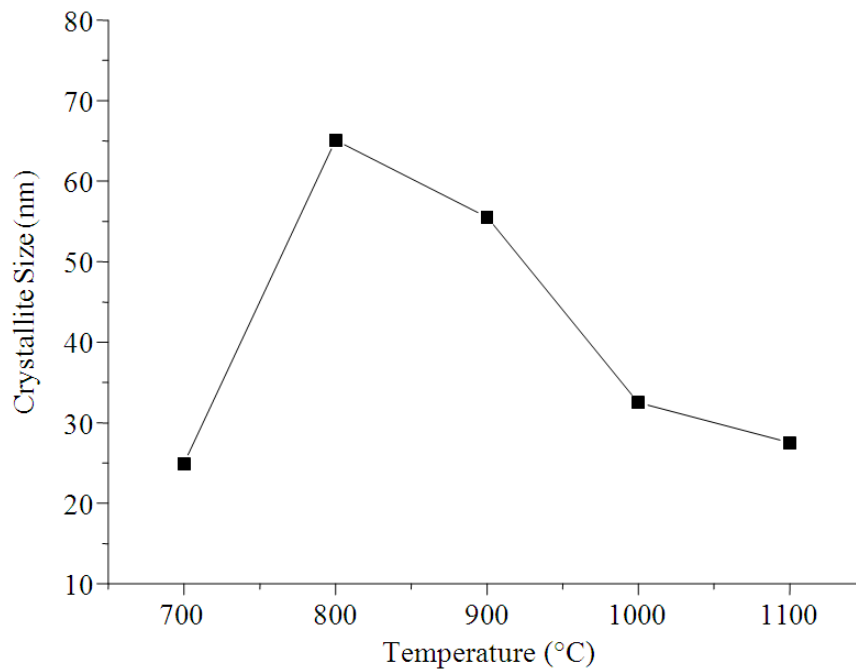


**Fig. 2.** Crystallite size of the Ni<sub>0.75</sub>Zn<sub>0.25</sub>Fe<sub>2</sub>O<sub>4</sub> at different calcinations temperatures

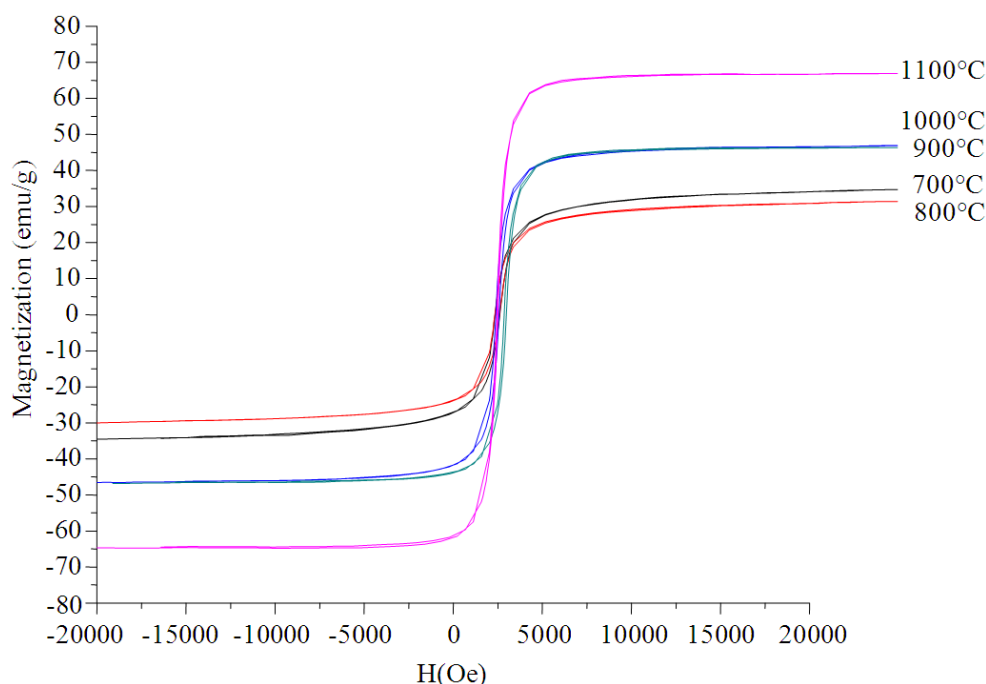


**Fig. 3.** Hysteresis curves of  $\text{Ni}_{0.75}\text{Zn}_{0.25}\text{Fe}_2\text{O}_4$  calcined at different temperatures

**Table 1.** Saturation magnetisation and coercivity values of  $\text{Ni}_{0.75}\text{Zn}_{0.25}\text{Fe}_2\text{O}_4$  calcined at different temperatures

Temperature (°C)	Saturation magnetization $M_s$ , (emu/g)	Coercivity $H_C$ , (Oe)
700	34.31	124.30
800	30.79	124.30
900	46.60	91.86
1000	46.60	63.22
1100	66.49	27.61

It can be attributed to the improvement of the crystallinity of the  $\text{Ni}_{0.75}\text{Zn}_{0.25}\text{Fe}_2\text{O}_4$  with the increase in calcination temperature which reduces the crystallite size.

At 700°C, the maximum saturation magnetization in applied field up to 20kOe is  $34.31 \text{ emu g}^{-1}$ . A slight decrease in maximum saturation magnetization from  $34.31 \text{ emu g}^{-1}$  to  $30.79 \text{ emu g}^{-1}$  was observed in the sample calcined at 800°C. The decrease in the maximum saturation magnetization can be attributed to a change in magnetic ordering in the  $\text{Ni}_{0.75}\text{Zn}_{0.25}\text{Fe}_2\text{O}_4$  due to the diminution of  $\text{Fe}_2\text{O}_3$  phase. Further increase in calcination temperature to 900°C, leads to the saturation of magnetisation starts to increase. It is due to the amount of the crystallinity phase increased as the calcination temperature increases. Evidently the intensity of the

major peak corresponds to  $\text{Ni}_{0.75}\text{Zn}_{0.25}\text{Fe}_2\text{O}_4$  increase with the increasing of calcination temperature as shown in **Fig. 1**. The coercivity values for  $\text{Ni}_{0.75}\text{Zn}_{0.25}\text{Fe}_2\text{O}_4$  samples were found to decrease with the calcination temperature (**Table 1**). The coercivity value varied from 124.30 Oe to 27.61 Oe. It was reported that saturation magnetization is related to coercivity through the Brown's relation (Xavier *et al.*, 2013). According to the theory, coercivity is inversely proportional to the saturation magnetization. As shown in **Table 1**, the saturation magnetization increased as calcination temperature increased. The variation of the saturation magnetization with temperature contributes to the decrease in coercivity.

#### 4. CONCLUSION

In conclusion, we have synthesized and studied the magnetic properties of  $\text{Ni}_{0.75}\text{Zn}_{0.25}\text{Fe}_2\text{O}_4$  samples at different calcination temperatures. Single  $\text{Ni}_{0.75}\text{Zn}_{0.25}\text{Fe}_2\text{O}_4$  phase can be obtained from 800 to 1100°C. At 800°C, the crystallite size of the sample starts to decrease with the increasing of calcination temperature. The saturation magnetization initially decreased due to the diminution of  $\text{Fe}_2\text{O}_3$  phase and

then increased with increasing calcination temperatures. The decrease in coercivity of the  $\text{Ni}_{0.75}\text{Zn}_{0.25}\text{Fe}_2\text{O}_4$  samples with calcination temperature can be attributed to the increase in the saturation magnetization. Although this study has provided a better understand of the influence of calcinations temperature on the magnetic properties of NiZn ferrite, however, the superexchange interactions and spin alignment at lattice sites in NiZn ferrite is still unclear. Future research might include the study of influence of calcinations temperature on the super-exchange interaction and spin alignment in NiZn ferrite.

## 5. ACKNOWLEDGEMENT

The financial support by Universiti Teknologi Petronas under Short Term Research Funding (STIRF) is greatly acknowledged.

## 6. REFERENCES

- Gao, P., H. Xia, V. Degirmencic, D. Rooney and M. Khraisheh *et al.*, 2013. Structural and magnetic properties of  $\text{Ni}_{1-x}\text{Zn}_x\text{Fe}_2\text{O}_4$  ( $x = 0, 0.5$  and  $1$ ) nanopowders prepared by sol-gel method. *J. Magnetism Magnetic Materials*, 348: 44-50. DOI: 10.1016/j.jmmm.2013.07.060
- Meng, Y.Y., Z.W. Liu, H.C. Dai, H.Y. Yu and D.C. Zheng *et al.*, 2012. Structure and magnetic properties of  $\text{Mn}(\text{Zn})\text{Fe}_{2-x}\text{RE}_x\text{O}_4$  ferrite nanopowders synthesized by co-precipitation and refluxing method. *Powder Technol.*, 229: 270-275. DOI: 10.1016/j.powtec.2012.06.050
- Sutka, A., A. Borisova, J. Kleperis, G. Mezinskis and D. Jakovlevs *et al.*, 2012. Paper: Effect of nickel addition on colour of nanometer spinel zinc ferrite pigments. *J. Aus. Ceramic Society*, 48: 150-155.
- Ismail, I., M. Hashim, I.R. Ibrahim, R. Nazlan and F.M. Idris *et al.*, 2013. Crystallinity and magnetic properties dependence on sintering temperature and soaking time of mechanically alloyed nanometer-grain  $\text{Ni}_{0.5}\text{Zn}_{0.5}\text{Fe}_2\text{O}_4$ . *J. Magnetism Magnetic Material*, 333: 100-107. DOI: 10.1016/j.jmmm.2012.12.047
- Vaqueiro, P., M.A. López-Quintela, J. Rivas and J.M. Grenèche, 1997. Annealing dependence of magnetic properties in nanostructured particles of yttrium iron garnet prepared by citrate gel process. *J. Magnetism Magnetic Materials*, 169: 56-68. DOI: 10.1016/S0304-8853(96)00728-7
- Beh, H.G., R. Irmawati, Y. Noorhana and K.P. Lim, 2009. Phase evolution and crystallite size of La-substituted YIG at different calcination temperatures. *Int. J. Eng. Technol.*, 09: 59-62.
- Islam, R., 2012. Effect of Sintering Temperature on structural and magnetic properties of  $\text{Ni}_{0.55}\text{Zn}_{0.45}\text{Fe}_2\text{O}_3$  ferrites. *Materials Sci. Applic.*, 3: 326-331. DOI: 10.4236/msa.2012.35048
- Pozo Lopez, G., A.M. Condo, S.E. Urreta, S.P. Silveti and M.D.C. Aguirre, 2012.  $\text{Ni}_{0.5}\text{Zn}_{0.5}\text{Fe}_2\text{O}_4$  nanoparticles dispersed in a  $\text{SiO}_2$  matrix synthesized by sol-gel processing. *Materials Characterisat.*, 74: 17-27. DOI: 10.1016/j.matchar.2012.08.010
- Cheng, Z.J., Y.M. Cui, H. Yang and Y. Chen, 2009. Effect of lanthanum ions on magnetic properties of  $\text{Y}_3\text{Fe}_5\text{O}_{12}$  nanoparticles. *J. Nanopart Res.*, 11: 1185-1192. DOI: 10.1007/s11051-008-9501-1
- Xavier, S., S. Thankachan, B.P. Jacob and E.M. Mohamed, 2013. Effect of sintering temperature on the structural and magnetic properties of cobalt ferrite nanoparticles. *Nanosyst.: Phys. Chem. Math.*, 4: 430-437.